

We are IntechOpen, the world's leading publisher of Open Access books Built by scientists, for scientists

6,900

Open access books available

185,000

International authors and editors

200M

Downloads

Our authors are among the

154

Countries delivered to

TOP 1%

most cited scientists

12.2%

Contributors from top 500 universities



WEB OF SCIENCE™

Selection of our books indexed in the Book Citation Index
in Web of Science™ Core Collection (BKCI)

Interested in publishing with us?
Contact book.department@intechopen.com

Numbers displayed above are based on latest data collected.
For more information visit www.intechopen.com



Evaluation of Non-condensable Gas Recirculation Flow in Steam Generator U-tubes during Reflux Condensation

Michio Murase¹, Takashi Nagae² and Noritoshi Minami²

¹*Institute of Nuclear Safety System, Incorporated,*

²*The Kansai Electric Power Company, Inc.
Japan*

1. Introduction

Under mid-loop operation during a PWR (pressurized water reactor) plant outage, reflux condensation in the SG (steam generator) U-tubes can be one of the major heat removal mechanisms in a hypothetical loss-of-RHR (residual heat removal systems) event. In mid-loop operation, the reactor coolant level is kept around the hot leg nozzle center and non-condensable gas (air or nitrogen) is present in the reactor coolant system (RCS). Such non-condensable gases are well known to accumulate on the condensation heat transfer surface and consequently inhibit steam from condensing. Therefore, in order to evaluate the effectiveness of reflux condensation in the SG U-tubes, the condensation heat transfer characteristics in the presence of a non-condensable gas must be clarified.

In the riser section of the SG U-tubes, the steam and non-condensable gas mixture and liquid condensate form countercurrent flow. A model for the influence of non-condensable gas on condensation was developed by Nithianandan et al. (1986) for the RELAP5/MOD2 code, based on an analogy between mass and heat transfers. However, the model was not well validated for countercurrent flow conditions while the condensation heat transfer coefficients in the presence of a non-condensable gas have been measured in many experiments, they have been measured very few times in countercurrent flow. Moon et al. (2000) measured the condensation heat transfer coefficients of steam-air mixtures in countercurrent flow, and proposed an empirical correlation as a degradation factor to the heat transfer coefficient of pure steam. Meanwhile Chun et al. (2001) placed a condenser tube bundle in a water pool and improved the empirical correlation by Moon et al. (2000). However, the correlations are limited to turbulent conditions of gas flow and when applied to laminar flow conditions, they overestimate the heat transfer coefficient.

Therefore, in our study, we carried out condensation heat transfer experiments in the presence of a non-condensable gas in a collaborative study at Purdue University (Vierow et al., 2003) and derived an empirical correlation mainly for laminar flow (Nagae et al., 2005). Moreover we conducted additional condensation heat transfer experiments, especially at high flow rates of a non-condensable gas, and improved the empirical correlation for turbulent flow conditions (Nagae et al., 2007a). In this article, we summarize the major results.

Using the BETHSY facility, which was a scale-model of a three-loop PWR, Noel & Deruaz (1994) and Noel & Dumont (1997) conducted reflux condensation tests. Different flow patterns were observed in the 34 U-tubes in the tests 7.2c with nitrogen injection (Noel & Deruaz, 1994), but were not observed in the tests 10.2 with helium injection (Noel & Dumont, 1997). In the test 7.2c-1.3 for example, an active condensation zone developed in the up-flow side of 21 U-tubes (active U-tubes), but nitrogen reverse flow from the outlet plenum to the inlet plenum occurred in some U-tubes (passive U-tubes).

In our study, we calculated steady-state flow patterns in U-tubes for the BETHSY tests 7.2c by one-dimensional analyses (Murase & Nagae, 2005) using a parallel channel model and the old correlation for condensation heat transfer coefficients by Nagae et al. (2005). In the steam-nitrogen mixture, density head is higher in the cold-side of active U-tubes than in the hot-side. In the region of low steam flow rates with small friction loss, the pressure becomes higher in the outlet plenum than in the inlet plenum, and nitrogen flows from the outlet plenum to the inlet plenum in passive U-tubes. About 10 solutions with different numbers of active U-tubes were obtained in our calculations. Using the assumption that the flow might be most stable in the case with the maximum nitrogen recirculation flow rate, we could obtain a unique solution for the number of active U-tubes, and the estimated number of active U-tubes agreed well with the BETHSY test results.

We also calculated different flow patterns in U-tubes (Nagae et al., 2007b) observed in the reflux condensation tests 7.2c by the BETHSY facility using the RELAP5/MOD3.2 code (The RELAP5 Development Team, 1995), where the improved correlation by Nagae et al. (2007a) for condensation heat transfer coefficients were applied. With modification of the equation for the interfacial and wall friction coefficients, nitrogen reverse flow was successfully calculated by RELAP5/MOD3.2, where SG U-tubes were modeled with two parallel flow channels. There were many solutions with different numbers of active U-tubes with condensation and the predicted number of active U-tubes agreed rather well with the measured values based on the assumption that the flow might be most stable in the case with the maximum nitrogen recirculation flow rate. In the calculations, however, the validity of the assumption has not been confirmed. Therefore, using RELAP5/MOD3.2 we calculated using three flow channels in order to change the flow area of active and passive U-tubes rather smoothly, and we evaluated the number of active U-tubes without the assumption (Minami et al., 2008). The ratio of active U-tubes calculated with three flow channels gave a good prediction of the ratio of active U-tubes. The results indicate the validity of the assumption that flow with the maximum nitrogen recirculation flow rate may be most stable and appear most probably among different numbers of active U-tubes. In this article, we also summarize the methods to predict the ratio of active U-tubes.

2. Heat transfer in the presence of non-condensable gas

In order to evaluate reflux condensation heat transfer characteristics in SG U-tubes in the presence of a non-condensable gas, experiments were conducted for condensation heat transfer of steam-air mixture under countercurrent flow in a vertical tube having an inside diameter of 19.3 mm and with pressure range from 0.1 to 0.4 MPa (Nagae et al., 2005 & 2007a).

2.1 Measurement methods

The design and manufacture of the experimental facility, experimental measurements, and data processing were done at Purdue University (Vierow et al., 2003). Figure 1 shows the experimental setup. Its main component was a vertical, double-pipe heat exchanger made of Type 304 stainless steel (SUS 304). The inner tube was the heat transfer tube with an inside diameter of 19.3 mm, wall thickness of 3.04 mm and a heat transfer length of 1.8 m. The mixture of steam and air flowed into the tube from the lower plenum. The coolant water flowed along the outer surface of the heat transfer tube.

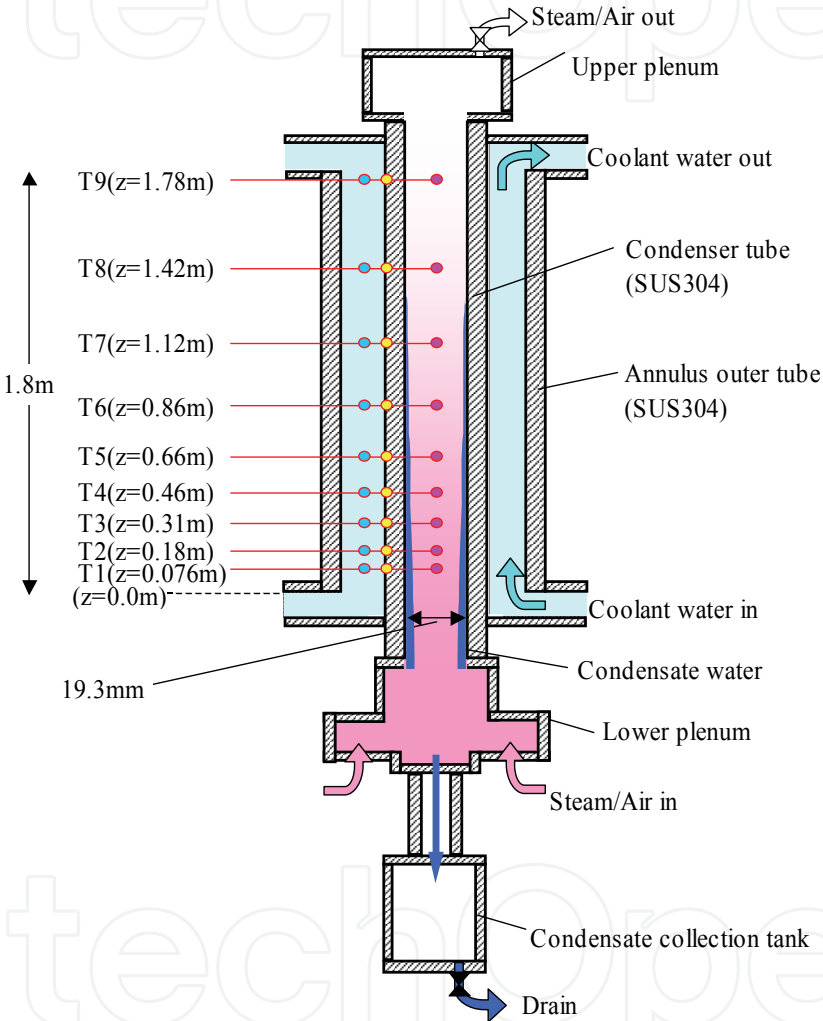


Fig. 1. Experimental setup (Vierow et al., 2003)

To obtain the condensation heat transfer coefficient under steady state conditions, the steam-air mixture temperature, outer wall temperature of the heat transfer tube, and coolant water bulk temperature were measured at nine elevations along the experimental section. The experimental conditions are listed in Table 1. The pressure, inlet steam mass flow rate, and air mass flow rate at the inlet of the test section were varied to examine their influence on the condensation heat transfer coefficient. The pressure and steam flow rate were selected based on the values presumed in the loss-of-RHR event during mid-loop operation. One objective of the experiment was to obtain a database under laminar and turbulent flow conditions.

Pressure (MPa)	0.1	0.2	0.4
Inlet conditions			
Steam mass flow rate (g/s)	0.49-1.9	1.1-1.9	0.48-1.9
Air mass flow rate (g/s)	0.03-0.18	0.06-0.5	0.06-0.8
Reynolds number of mixture	2900-10000	6500-10000	3100-9500
Measured regions			
Steam mass flow rate (g/s)	0.00031-1.9	0.00039-1.9	0.00020-1.9
Partial pressure ratio, P_{steam}/P_{air}	0.027-120	0.012-47	0.0054-49
Reynolds number of mixture	73-10000	210-10000	210-9500

Table 1. Experimental conditions

In the experiment, the temperature of the steam-air mixture, T_g , and the outer wall temperature of the heat transfer tube, $T_{w,o}$, were measured, and the heat flux at the inner surface of the heat transfer tube, q'' , and the overall heat transfer coefficient, K , were defined by the following equations:

$$q'' = K(T_g - T_{w,o}) \tag{1}$$

$$\frac{1}{K} = \frac{r_{w,i} \ln(r_{w,o}/r_{w,i})}{\lambda_w} + \frac{1}{h_c} \tag{2}$$

where $r_{w,i}$ is the inner radius of the heat transfer tube, $r_{w,o}$ is the radius of the thermocouple location to measure outer wall temperature of the heat transfer tube, λ_w is the thermal conductivity of the heat transfer tube, and h_c is the condensation heat transfer coefficient. The first term on the right hand side of Eq. (2) can be calculated from the dimensions and physical properties of the heat transfer tube. Accordingly, the condensation heat transfer coefficient, h_c , can be calculated once the heat flux is known.

From the coolant temperature variation, the mean heat flux q'' between the measured sections in Eq. (1) can be calculated. Since the coolant temperature variation is small in the downstream region of the heat transfer tube, where both the condensation rate and measurement accuracy are low, the mean heat flux between the measured sections is calculated from the temperature variation of the steam-air mixture. Temperature measurements provide the local saturation pressure, and the steam mass flow rate can be calculated from the partial pressure of steam, $P_{steam}(T_g)$, assuming a Gibbs-Dalton mixture of steam and an ideal non-condensable gas. Then the local heat flux can be obtained (for details, see Nagae et al., 2005 & 2007a).

In Eq. (2), the condensation heat transfer coefficient consists of the heat transfer coefficient of the liquid film, h_f , and the heat transfer coefficient at the gas-liquid interface, h_i , which are separately evaluated in this study, because they are different heat transfer mechanisms. When the effects of the liquid film subcooling and the liquid film thickness on the gas-liquid interface area can be neglected, the condensation heat transfer coefficient is expressed by:

$$\frac{1}{h_c} = \frac{1}{h_f} + \frac{1}{h_i} \tag{3}$$

According to the calculations, the subcool enthalpy of the liquid film is about 3% of the condensation enthalpy, and the gas-liquid interface area is about 99% of the inner surface area of the heat transfer tube under the experimental conditions. In Eq. (3), the heat transfer coefficient of the liquid film, h_f , can be calculated by Nusselt's film condensation theory or an empirical correlation for a turbulent film such as the correlation modified by McAdams (1954), which we use in this study. Then, the interfacial heat transfer coefficient, h_i , is obtained from the measured condensation heat transfer coefficient, h_c .

2.2 Interfacial heat transfer coefficients

Important parameters for the interfacial heat transfer coefficients, h_i , are properties of a non-condensable gas and gas velocity. The effects of a non-condensable gas were evaluated by Nagae et al. (2005), and mass flow ratio of (W_{steam}/W_{air}) and pressure ratio of (P_{steam}/P_{air}) gave similar results. In the transient analysis, mass flow rates sometimes fluctuate and pressures are more stable than mass flow rates. Therefore the pressure ratio of (P_{steam}/P_{air}) is adopted in this study. As for gas velocity, steam Reynolds number gave better results than steam-air mixture Reynolds number for limited data (Nagae et al., 2005). However, steam Reynolds number is not suitable for the additional data (Nagae et al., 2007a). Therefore, the empirical correlation for the interfacial heat transfer coefficient was reevaluated using the Reynolds number of the steam-air mixture, Re_g . The same function of (P_{steam}/P_{air})^{0.75} for laminar flow (Nagae et al., 2005) is used for turbulent flow, and the constants a and exponent b for Re_g are determined by the least mean square method. The modified empirical correlation by Nagae et al. (2007a) is as follows:

$$Nu_i = \frac{h_i d_{w,i}}{\lambda_g} = 120 \left(\frac{P_{steam}}{P_{air}} \right)^{0.75} \max(1.0, a Re_g^b) \quad (4)$$

with $Re_g = \frac{j_g d_{w,i}}{\nu_g} \leq 10,000$, $a = 0.0035$, $b = 0.8$,

where j_g is the superficial velocity of the steam-air mixture and ν_g is the viscosity of the steam-air mixture. In order to apply Eq. (4) to the transient analysis codes, where empirical correlations are often used beyond their application limits, the following limits are suggested:

$$Nu_i = \frac{h_i d_{w,i}}{\lambda_g} \geq 4.36, \quad 0.0054 \leq \frac{P_{steam}}{P_{air}} \leq 120, \quad Re_g = \frac{j_g d_{w,i}}{\nu_g} \leq 10,000, \quad (5)$$

where the lower limit of the Nusselt number corresponds to the heat transfer of a gas laminar flow without steam condensation and gives about $h_f = 7$ W/m²K. Other limits are the measured region listed in Table 1.

Figure 2 compares the interfacial heat transfer coefficients calculated by Eq. (4) with measured values (Nagae et al., 2005 & 2007a). The calculated results agreed well with the data in a wide range of heat transfer coefficients. In the region of large heat transfer coefficients, however, the points were scattered because the measured values scattered near the entrance of the experimental section due to a small increase in the cooling water temperature.

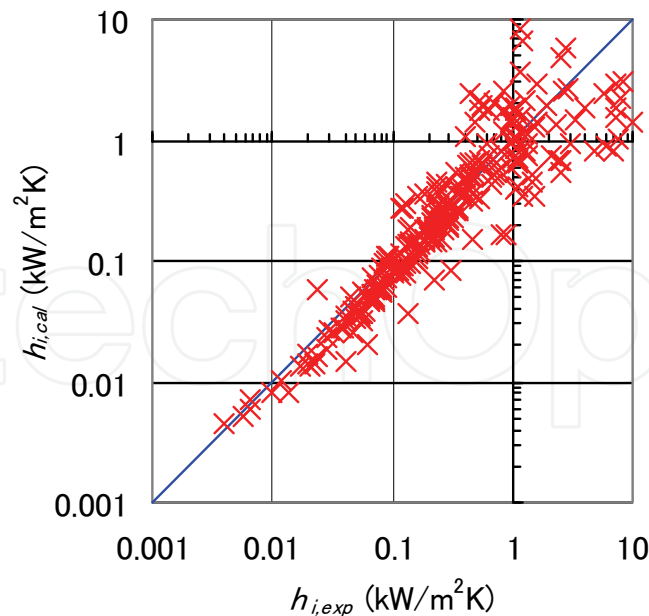


Fig. 2. Comparison of interfacial heat transfer coefficients, $h_{i,cal}$, calculated by Eq. (4) with data, $h_{i,exp}$

2.3 Experimental analyses by RELAP5/MOD3.2 with modified correlation

Figure 3 shows the nodalization scheme of RELAP5/MOD3.2 for calculations of the condensation heat transfer experiments shown in Fig. 1. The nodalization scheme contains 125 control volumes, 7 junctions, and a valve and heat structure. Both the steam-air mixture and coolant were injected at constant flow rates upward into the heat transfer tube and along the outer surface of the tube, respectively. In the calculation, this behavior is simulated using a volume and a junction to specify flow, pressure and temperature conditions. Volumes act as infinite sources or sinks and represent boundary conditions. Volume 100 is connected to Pipe 110, which represents the lower plenum with a junction. Junction 115 connects Pipe 110 with the inlet of Pipe 140, which represents the inlet pipe and measurement section. Junction 141 connects the outlet of Pipe 140 with Pipe 142, which represents the upper plenum. Valve 175 is used to regulate the venting of the residual steam-air mixture to the atmosphere. Junction 159 connects Pipes 156 and 160 that simulate a condensate water line and a collection tank. Volumes 200 and 280 are connected to Pipe 240, which represents the coolant water line, with Junctions 210 and 270, respectively. Heat structure 140 with 55 sub-volumes is used to represent the heat transferred from the steam-air mixture to the coolant through the heat transfer tube.

Figure 4 shows the axial temperature profiles (Nagae et al., 2007a). Using the default model correlation by Nithianandan et al. (1986) gave much higher mixture temperatures especially for a high pressure condition. It seemed that the default vapor-diffusion model through the non-condensable gas layer underestimated heat transfer coefficients especially for high pressures. On the other hand, the temperature distribution of the steam-air mixture calculated by RELAP5/MOD3.2 with the modified correlation agreed well with the data. The calculations overestimated the outer surface temperatures of the tube near the inlet in all cases. The reason might be the high heat transfer coefficient outside the heat transfer tube near the inlet due to the entrance effect in the experiments.

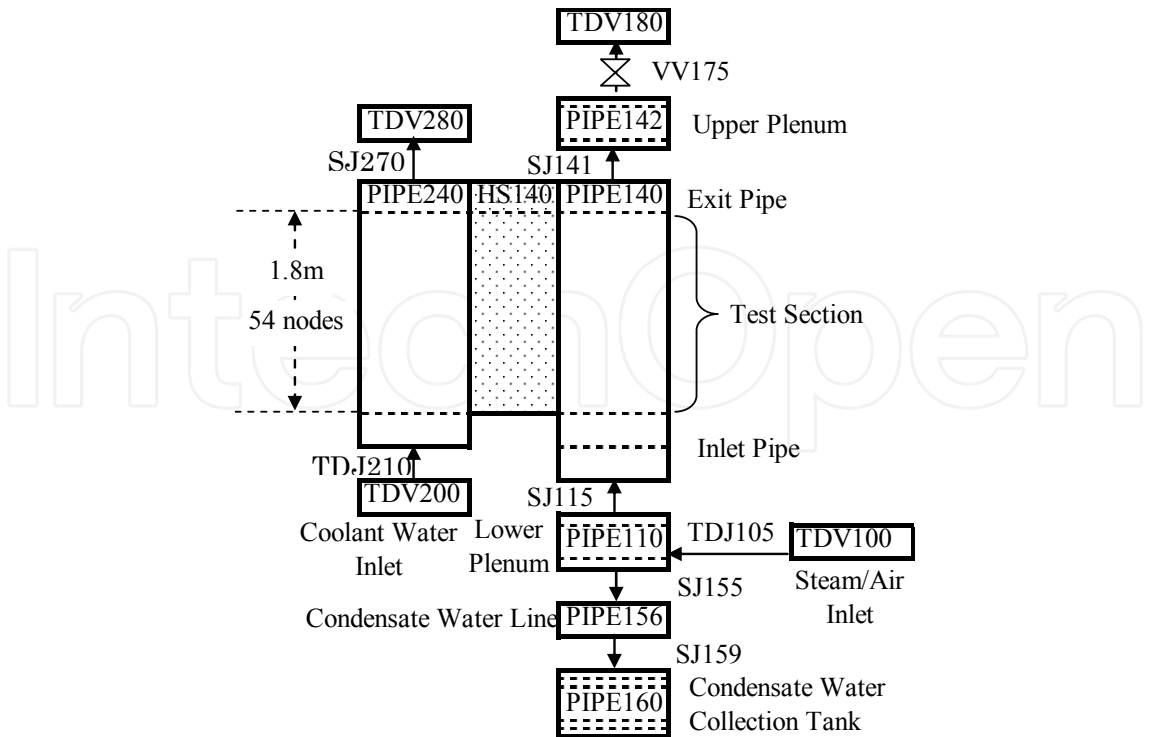


Fig. 3. Nodalization for calculations using RELAP5/MOD3.2

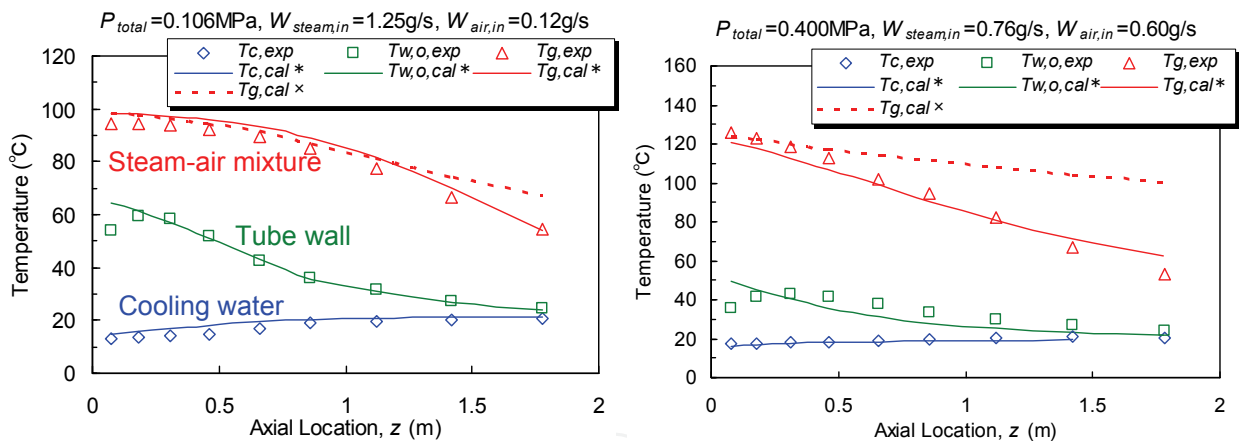


Fig. 4. Comparison of axial temperatures (exp: measured data; calx: RELAP5-default model correlation; cal*: RELAP5-modified correlation)

3. Steady-state calculations of BETHSY tests 7.2c

In order to evaluate the mechanism of different flow patterns observed in the BETHSY tests 7.2c (Noel & Deruaz, 1994), steady-state calculations were conducted using a parallel channel model (Murase & Nagae, 2005; Nagae et al., 2007b).

3.1 Reflux tests in BETHSY facility

The BETHSY facility is a scale-model of a three-loop 900 MWe PWR with the full height and 1/100 of the volume, flow rate and power level. Each SG has 34 U-tubes with the inner diameter of 19.68 mm and the average length of 19.45 m.

The conditions and major results of the reflux tests 7.2c (Noel & Deruaz, 1994) are listed in Table 2. In the tests, one loop was used and the other two loops were isolated. The power in the core was constant at about 98 kW, which simulated about 0.33 % of the rated power and generated the steam flow rate of 47 g/s (1.38 g/s/U-tube). The secondary-side pressure of the SG was constant at 0.2 MPa. A test was started with pure steam, and nitrogen was injected gradually into the vertical part of the hot leg upstream of the SG inlet plenum. The injected nitrogen flowed into the U-tubes and accumulated in the SG outlet plenum and the cold leg, which was sealed with coolant water in the crossover leg. The primary pressure increased gradually during injection of nitrogen, and reached a constant value after the termination of the injection. Table 2 shows the primary pressure and the number of active U-tubes at a steady state after the termination of the nitrogen injection. The temperatures in the inlet of the 34 U-tubes were measured, and it seemed that U-tubes with a temperature close to the inlet plenum temperature and U-tubes with a temperature close to the outlet plenum temperature would be evaluated as active U-tubes with steam condensation and passive U-tubes with a nitrogen reverse flow, respectively.

	Test conditions				Results	
Test No.	Q_{core} (kW)	P_2 (MPa)	Gas	M_{NG} (kg)	P_1 (MPa)	N_{act}
7.2c-1.1	97.0	0.2	None	0.0	0.23	34
7.2c-1.2	98.5	0.2	N ₂	0.32	0.38	24
7.2c-1.3	98.5	0.2	N ₂	0.65	0.55	21
7.2c-1.4	99	0.2	N ₂	1.08	0.78	19

Table 2. Test conditions and major results of the BETHSY tests 7.2c (Noel & Deruaz, 1994); M_{NG} : mass of injected nitrogen; N_{act} : number of active U-tubes; P_1 and P_2 : pressure of primary and secondary loops, respectively; Q_{core} : core power

3.2 Calculation model

In this study, we did calculations for the steady state after the termination of the nitrogen injection in the tests 7.2c, where different flow patterns appeared. Flow patterns in U-tubes are illustrated in Fig. 5. We assumed that there were active U-tubes with steam condensation and passive U-tubes with a nitrogen reverse flow, and the one-dimensional flow in the axial direction was calculated accordingly. In the calculation of thermal-hydraulics in a single U-tube, the temperature distribution of the steam-nitrogen mixture and the pressure drop between the inlet and outlet plenums were calculated while varying the steam flow rate or nitrogen flow rate as a parameter. In the calculation of thermal-hydraulics in parallel U-tubes, the number of active U-tubes was fixed at one value, the temperature distributions and the pressure drops in active and passive U-tubes were calculated varying the nitrogen recirculation flow rate as a parameter, and the solution with the same pressure drop between active and passive U-tubes was obtained.

The pressure drop between the inlet and outlet plenums could be expressed by the equation:

$$P_{in} - P_{out} = \frac{\zeta_{in}}{2}(\rho_m |j_m| j_m)_{in} + \int_0^L \rho_m \left(\frac{f}{2d_i} |j_m| j_m + g \right) dz + \frac{\zeta_{out}}{2}(\rho_m |j_m| j_m)_{out} \tag{6}$$

where ρ_m and j_m are the density and superficial velocity of the steam-nitrogen mixture, respectively. j_m and dz are positive in the region of $0 < z < L/2$, but negative in the region of

$L/2 < z < L$, where L is the length of the U-tube. Inlet pressure loss coefficient of $\zeta_{in} = 0.5$ without curvature at the corner and outlet pressure loss coefficient of $\zeta_{out} = 1.0$ for sudden expansion were used. The friction loss coefficient, f , for an annular flow by Wallis (1969) was used.

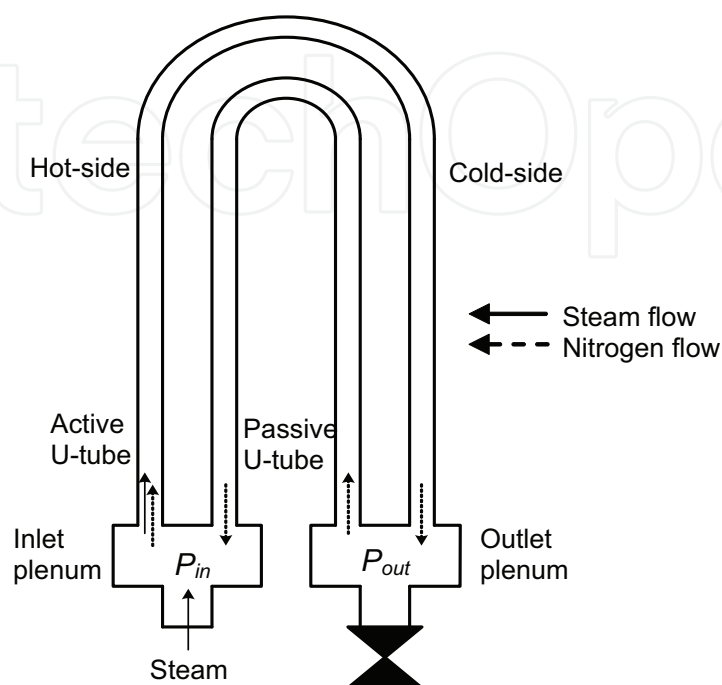


Fig. 5. Calculation model of flow patterns in U-tubes

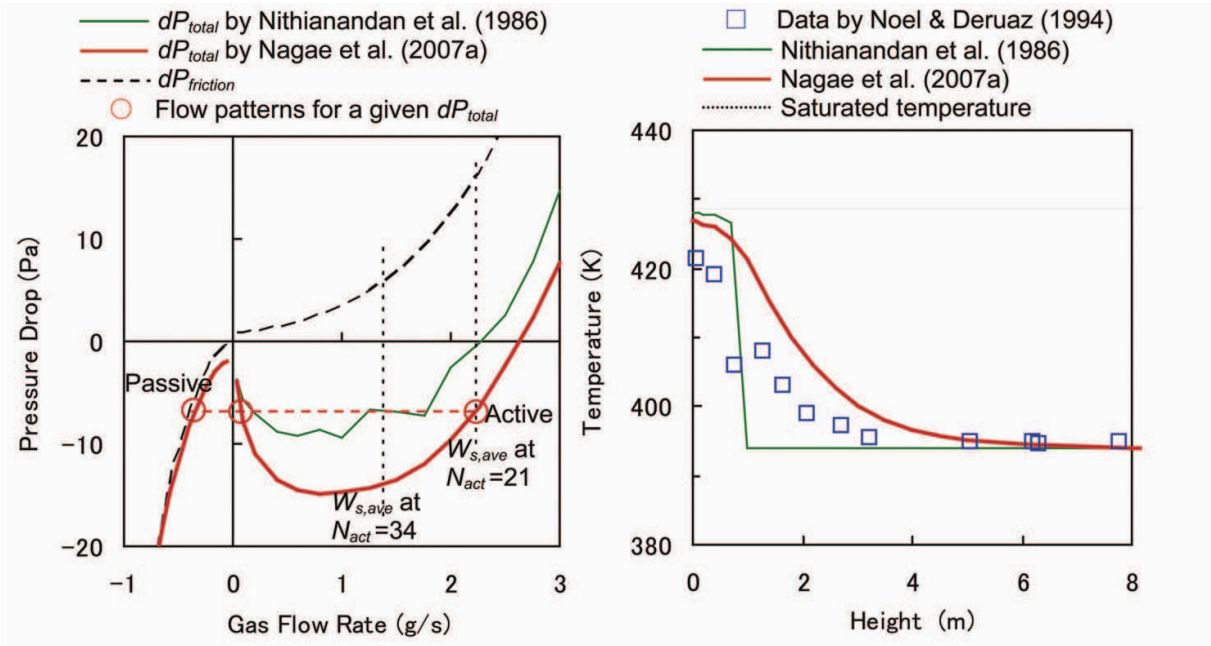
The density of the steam-nitrogen mixture, ρ_m , was a function of the pressure and temperature. Steam pressure could be calculated by applying Dalton's law and ideal gas law to nitrogen. The temperature of the steam-nitrogen mixture was calculated from the steam partial pressure by assuming a saturated state of steam. The steam flow rate could be calculated by the heat transfer equations, where the heat transfer coefficient outside the U-tube was calculated by the maximum value of the laminar flow heat transfer at low superheating and the pool nucleate-boiling heat transfer by Kutateladze at high superheating, and the condensation heat transfer coefficient was calculated using Eqs. (3) and (4) (for details, see Nagae et al., 2007b).

3.3 Pressure drop and axial temperature distribution

Figure 6 (a) shows calculated pressure drop in a single U-tube for the test 7.2c-1.3. Positive and negative gas flow rates represent those of steam and nitrogen, respectively. It should be noted that Fig. 6 (a) shows an example of pressure drop characteristics; the actual pressure drop changed depending on the number of active U-tubes and nitrogen recirculation flow rate. Friction loss, $dP_{friction}$, in the figure included inlet and outlet pressure losses in Eq. (6) and the difference between the total pressure drop, dP_{total} , and friction loss was the term of density head. Because density head was larger in the cold-side than in the hot-side, the pressure drop between inlet and outlet plenums became negative in the region of low flow rates with small friction loss. Correlations of the condensation heat transfer coefficient affected temperature and density head. The calculated pressure drop using the correlation

by Nithianandan et al. (1986) did not change smoothly, which may be due to the rapid change of heat transfer coefficients from turbulent flow to laminar flow. However, its effect was several Pa and small compared with the differential pressures in the hot-side and cold-side of about 400 Pa.

In the test 7.2c-1.3, the average steam flow rate per U-tube was $W_{s,ave}=1.38$ g/s and the steam flow rate per U-tube in the case of 21 active U-tubes ($N_{act}=21$; see Table 2) became 2.24 g/s. In the U-tube bundle, the pressure drop of each U-tube became equal, and three patterns (three open circles in Fig. 6 (a)), active U-tubes, passive U-tubes and U-tubes with low steam flow rate, may appear for a given pressure drop. However, it is well known that the flow pattern with a negative pressure drop gradient is unstable and may not appear in parallel channels (Ozawa, 1999). Therefore, in this study, we considered active U-tubes and passive U-tubes in the following calculations.



(a) Calculated pressure drop (test 7.2c-1.3) (b) Axial temperature distribution ($N_{act} = 21$)

Fig. 6. Results of steady-state calculations (N_{act} : number of active U-tubes)

Figure 6 (b) compares measured and calculated temperatures of steam-nitrogen mixture in active U-tubes. In the calculations, the measured number of active U-tubes, $N_{act}=21$, was used. Changing the nitrogen recirculation flow rate as a parameter, we calculated pressure drops of active and passive U-tubes, and a solution with the same pressure drops between the active and passive U-tubes was obtained.

In the calculation using the correlation by Nithianandan et al. (1986), as shown in Fig. 6 (a), the pressure drop was nearly zero at $N_{act}=21$ and the nitrogen reverse flow rate in the passive U-tube was quite low. Therefore, almost pure steam entered the active U-tube and the temperature of the mixture decreased rapidly due to steam condensation. On the other hand, in the calculation using the correlation by Nagae et al. (2007a), the nitrogen reverse flow rate in the passive U-tube was large, condensation heat transfer coefficients became low due to the non-condensable gas, and the temperature of the mixture decreased gradually. The temperatures calculated using the correlation by Nagae et al. (2007a) were overestimated, but showed good agreement with the trend of the measured temperatures.

3.4 Prediction of number of active U-tubes

Under the countercurrent gas-liquid flow in vertical parallel channels between upper and lower plenums, where gas is supplied to the lower plenum and liquid is supplied to the upper plenum, the pressure drop between the upper and lower plenums has a similar trend to the pressure drop shown in Fig. 6 (a), and gas up-flow and liquid down-flow appear in parallel channels (Wallis et al., 1981; Murase & Suzuki, 1986). In this case, the flow pattern with the minimum pressure drop is the most stable among several flow patterns and appears most easily (Murase & Suzuki, 1986). In the vertical parallel channels, however, the gas flow rate and the pressure drop are positive, which are different from those in the U-tubes shown in Fig. 6 (a) where the pressure drop was negative. In the long U-tubes, the steam flow rate generated by decay heat was low compared with the large heat transfer area. Therefore, we assumed that the flow might be most stable in the case with the maximum nitrogen recirculation flow rate, and the predicted number of active U-tubes using the assumption agreed well with the BETHSY test results (Murase & Nagae, 2005).

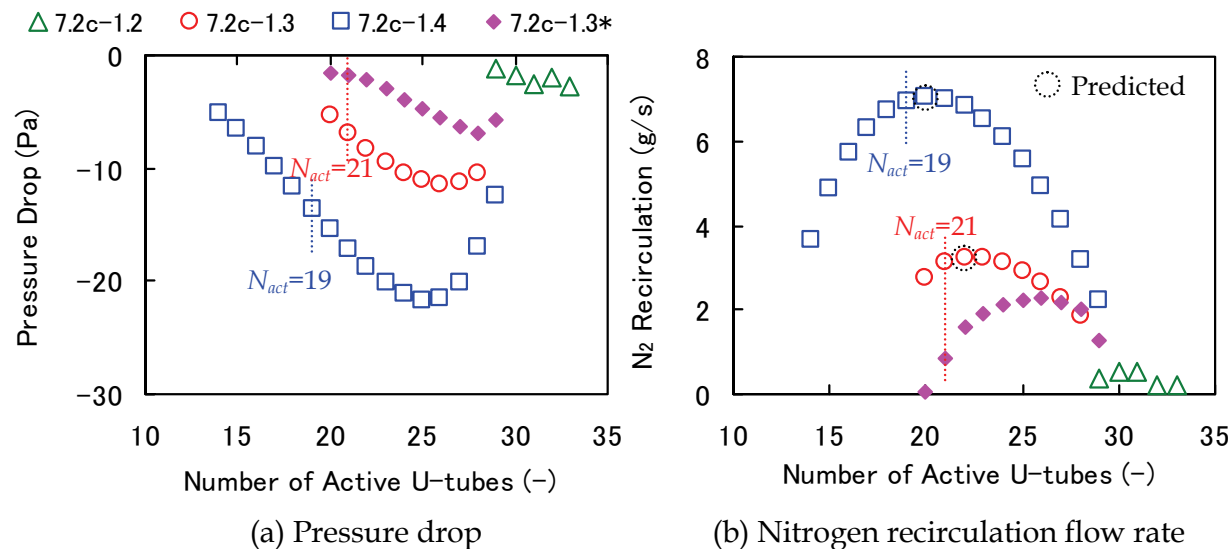


Fig. 7. Results calculated for 34 U-tubes; N_{act} : number of active U-tubes observed by Noel & Deruaz (1994); *condensation heat transfer correlation by Nithianandan et al. (1986); others: condensation heat transfer correlation by Nagae et al. (2007a)

Figure 7 shows calculated pressure drop and nitrogen recirculation flow rate (Nagae et al., 2007b). As the injected mass of nitrogen increased, nitrogen recirculation flow rate increased and the pressure difference between the inlet and outlet plenums (absolute value of the pressure drop of U-tubes) became large. By assuming that the flow might be most stable in the case with the maximum nitrogen recirculation flow rate, the predicted numbers of active U-tubes agreed well with the measured values except for 7.2c-1.2. In order to predict the number of active U-tubes, $N_{act}=24$ in 7.2c-1.2, an accurate pressure drop calculation is required. In the case of 7.2c-1.4, the predicted number of active U-tubes was 20 for the measured value of $N_{act}=19$. The differences of calculated temperatures in the cases of $N_{act}=18$ to 20 were small and less than 2 K. Figure 7 (b) also shows that the condensation heat transfer correlation was important to predict the number of active U-tubes, because the pressure drop between the inlet and outlet plenums was very small as shown in Fig. 7 (a).

4. Transient calculations using RELAP5/MOD3.2

4.1 Calculation model and conditions

In the transient calculations of the BETHSY tests 7.2c, RELAP5/MOD3.2 was used (Nagae et al., 2007b; Minami et al., 2008), where the correlation of condensation heat transfer was modified using Eq. (4). In the transient analyses, SG U-tubes are generally modeled by a single flow channel, but they must be modeled by multiple flow channels for the calculation of the nitrogen reverse flow from the outlet plenum to the inlet plenum, so we modeled SG U-tubes by two or three flow channels.

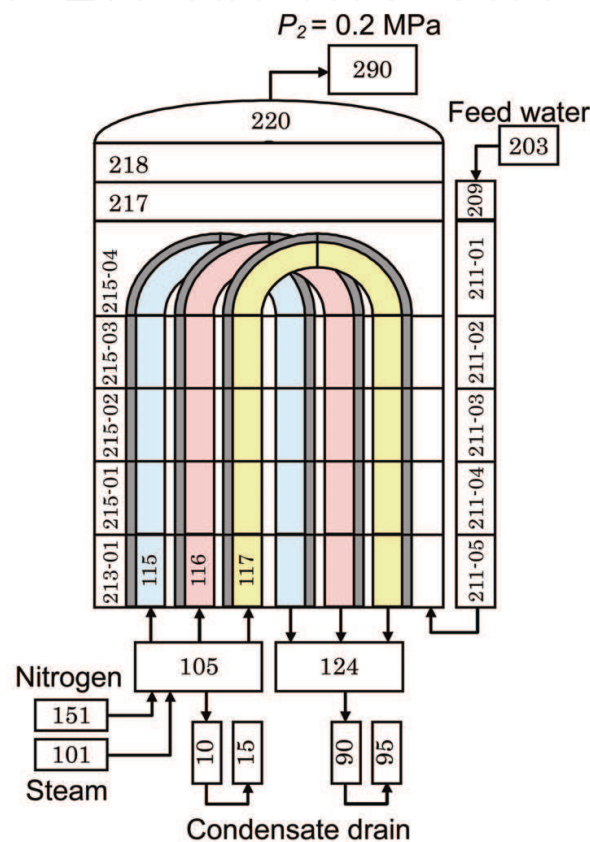


Fig. 8. Nodalization for calculations by RELAP5/MOD3.2

Figure 8 shows the nodalization scheme of the SG of the BETHSY tests with three flow channels, Volumes 115, 116 and 117. In the case of two flow channels, Volumes 115 and 116 were used. The nodalization used for these calculations included control volumes, junctions and heat structures. Volume 101 simulated the steam flow rate generated in the core. Volume 151 simulated the nitrogen flow injected into the hot leg. Volumes 10 and 15, and 90 and 95 were connected to the inlet plenum and the outlet plenum, respectively, in order to drain the condensate water, since the change in free volume would affect the calculations. The water level in the secondary side of the SG was kept constant by feed water from Volume 203. The pressure in the secondary side was kept at 0.2 MPa. The inner diameter of U-tubes was 19.68 mm, and the length of U-tubes was 17.98, 19.45 or 20.92 m. In Fig. 8, the average length of 19.45 m was used for the three flow channels, Volumes 115, 116 and 117, because the difference of pressure drops calculated for 17.98, 19.45 and 20.92 m was smaller than 1 Pa (Murase & Nagae, 2005).

The volume of the inlet and outlet plenums is about 0.035 m³ in the BETHSY facility (Bazin, 1988), but is about 0.05 m³ in the same scale model of a Japanese typical PWR plant. The volume of the inlet and outlet plenums does not directly affect thermal-hydraulic behavior, but the important parameter is the gas volume in the outlet plenum and cross-over leg, which affects the partial pressure of nitrogen there. According to the calculation by Murase & Nagae (2005) using the one-dimensional parallel channel model, the gas volume of the outlet plenum was about 0.02 m³, which was obtained from the mass of injected nitrogen and measured pressure of the primary loop in the BETHSY tests. Therefore, we used the volume of 0.02 m³ for the base case or 0.05 m³ for a parameter calculation to evaluate its effect.

4.2 Modification of calculation equation

At first, a transient calculation was conducted using two flow channels with the flow area ratio of 21:13. Both flow channels were active in test 7.2c-1.1 without nitrogen injection, and the gas flow rate ratio and heat transfer ratio between Volumes 115 and 116 were almost the same as their flow area ratio (i.e. number ratio of U-tubes). After nitrogen injection, the calculated gas flow rates and heat transfer rates in Volumes 115 and 116 repeated out-of-phase oscillations and nitrogen reverse flow was not calculated. Moreover, the calculated steam velocities in the test 7.2c-1.1 were different by about 0.5 % between Volumes 115 and 116, which was small as a calculated result but large as a calculation error. We found that the gas-liquid interfacial friction forces between Volumes 115 and 116 were different by about 5%. Therefore, we checked calculation equations of the interfacial friction force. In RELAP5, the node and junction method, where pressure is defined at the center of each volume and velocity is defined at each junction, is used. And in the calculation of pressure drop between volumes, the following weighting factor is used for calculations of the interfacial friction force and the wall friction force.

$$\frac{A_j(j)}{A_v(i)} \cdot \frac{0.5L_v(i)}{0.5L_v(i) + 0.5L_v(k)} + \frac{A_j(j)}{A_v(k)} \cdot \frac{0.5L_v(k)}{0.5L_v(i) + 0.5L_v(k)} \quad (7)$$

where A_j is flow area of a junction, A_v is flow area of a volume, L_v is length of a volume, and (i) and (k) show the upstream and downstream volumes of the junction, respectively. It is not clear why the flow area ratio (A_j / A_v) is used in Eq. (7), but it is clear that Eq. (7) gives different forces for the U-tube volumes because flow areas of the junctions A_j (j) for Volumes 115 and 116 are 21:13. Therefore, Nagae et al. (2007b) modified Eq. (7) to:

$$\left[\frac{D_j(j)}{D_v(i)} \right]^2 \cdot \frac{0.5L_v(i)}{0.5L_v(i) + 0.5L_v(k)} + \left[\frac{D_j(j)}{D_v(k)} \right]^2 \cdot \frac{0.5L_v(k)}{0.5L_v(i) + 0.5L_v(k)} \quad (8)$$

where D_j is the hydraulic diameter of a junction and D_v is the hydraulic diameter of a volume. We used Eq. (8) to minimize the modification of Eq. (7) and to keep $(A_j / A_v) = (D_j / D_v)^2$ for a circular tube because its effects on the other configurations are not clear.

In the case of 17:17, for example, the interfacial friction force and the wall friction force of the inlet plenum should be about 0.13 % of those of the U-tube inlet section. However, the first term of Eq. (7) gave about 13.5 % of the second term of Eq. (7). This meant that Eq. (7) gave large interfacial force and wall friction force. The first term of Eq. (8) gave about 0.01 % of the second term of Eq. (8), which was smaller than 0.13 % mentioned above. However, its effect on the calculated values of the interfacial force and wall friction force was negligibly small.

4.3 Transient calculations with two flow channels

Figure 9 shows the calculated gas flow rate at the inlet of SG U-tubes and pressure at the SG inlet plenum (Nagae et al., 2007b), where Eq. (8) was used for calculations of the interfacial friction force and wall friction force. In the two flow channels, their number of U-tubes are 21 and 13 for Volumes 115 and 116, respectively. The volume of inlet and outlet plenums is 0.02 or 0.05 m³.

The gas flow rate ratio between Volumes 115 and 116 were the same as their flow area ratio (i.e. number ratio of U-tubes) of 21:13. After nitrogen injection, the pressure drop became negative, and the gas flow rate of Volume 115 increased. On the other hand, the gas flow rate of Volume 116 became negative (reverse flow). Nitrogen flowed from the outlet plenum to the inlet plenum in Volume 116 and recirculated into Volume 115. Two flow channels separated into active U-tubes (Volume 115) and passive U-tubes (Volume 116) in the calculations. Special thermal-hydraulic models and input data were not used for Volumes 115 and 116, and it seemed that the calculated results approached the more stable solution due to some disturbance in the calculation. In tests 7.2c-1.3 and 7.2c-1.4, Volume 115 and Volume 116 remained active and passive, respectively. As the injected nitrogen increased, the gas flow rate of Volume 115 increased because nitrogen reverse flow increased in Volume 116 and recirculated into Volume 115. The heat transfer rate in passive U-tubes was only about 0.3% of the whole heat transfer rate.

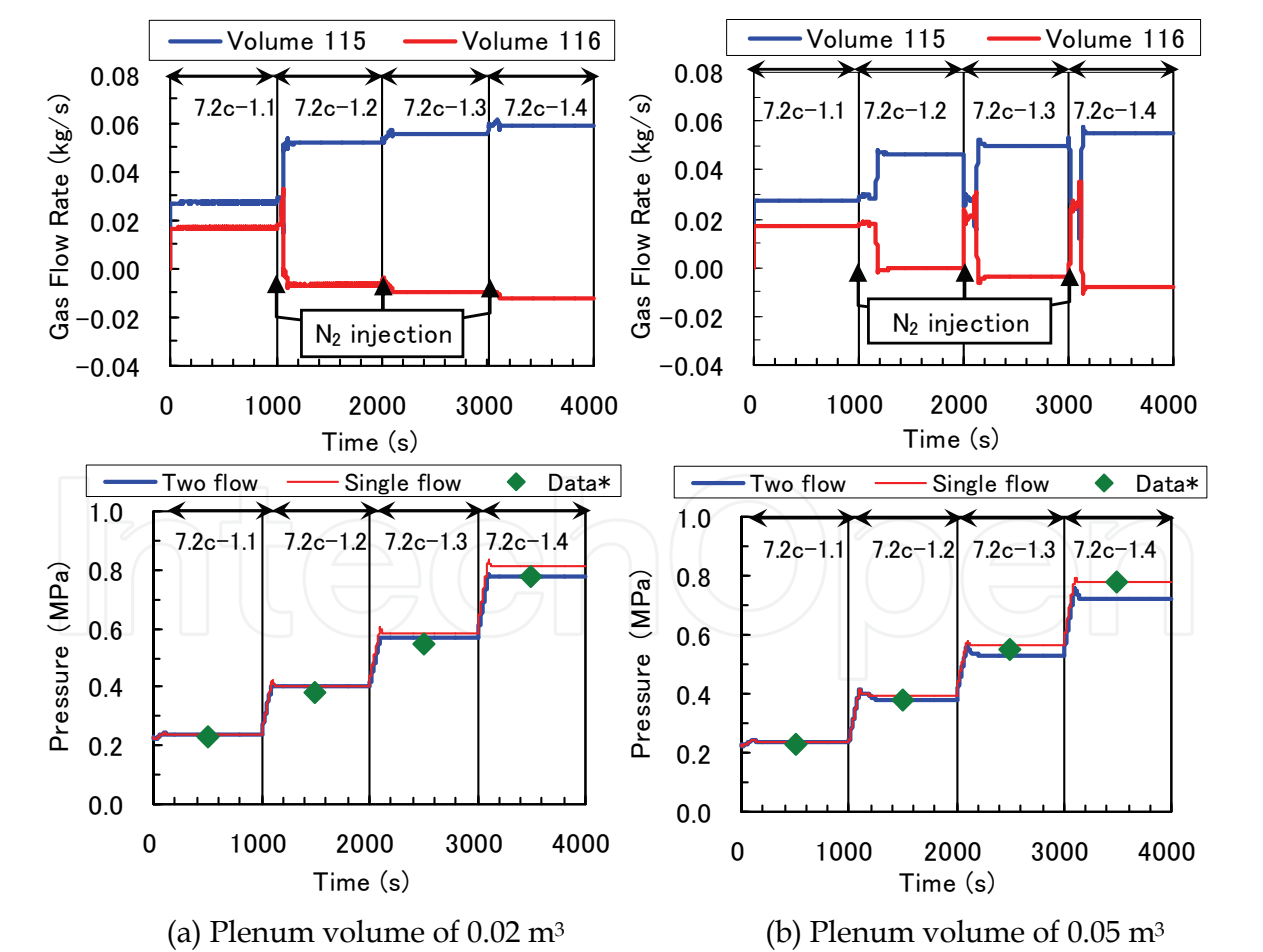


Fig. 9. Results calculated by RELAP5/MOD3.2 using two flow channels with 21 and 13 U-tubes; *Data: Noel & Deruaz (1994)

The calculated results were similar between the plenum volumes of 0.02 and 0.05 m³, except for the behavior during the nitrogen injection and the pressure at the SG inlet plenum. The nitrogen reverse flow continued in the case with the plenum volume of 0.02 m³, but terminated during the nitrogen injection in the case with the plenum volume of 0.05 m³. Pressures calculated with the two flow channels were a little lower than those calculated with the single flow channel, but the differences were small because the steam condensation zone was much shorter than the U-tube length and the inlet and outlet plenum volume was small, and the calculated pressures of both cases agreed well with the measured values. Figure 9 results indicated that the volume of the SG inlet and outlet plenums with non-condensable gas affected the pressure at the SG inlet plenum and stability of the calculations.

Figure 10 shows the nitrogen recirculation flow rate and the SG inlet plenum pressure versus the number of active U-tubes as the calculation parameter (Nagae et al., 2007b).

In the steady state calculations, assuming that the flow might be most stable in the case with the maximum nitrogen flow rate, a unique solution for the number of active U-tubes could be obtained, and the estimated number of active U-tubes agreed well with observed results except 7.2c-1.2, as shown in Fig. 7 (b). Therefore, similar calculations were performed using RELAP5/MOD3.2. Figure 10 (a) shows nitrogen recirculation flow rates calculated changing the flow area ratio of U-tube Volumes 115 and 116. In the calculations, the flow area ratio of U-tubes changed from 17:17 to 33:1. In the calculations, active U-tubes with condensation and passive U-tubes with the nitrogen reverse flow appeared even in the calculations for 7.2c-1.2, and the horizontal axis in Fig. 10 shows the number of active U-tubes as calculated results. In the case of the plenum volume of 0.02 m³, active U-tubes appeared in the flow channel with large flow area in all calculations and the nitrogen reverse flow was calculated in the region of $N_{act} \geq 17$. The results underestimated the number of active U-tubes with the maximum nitrogen recirculation flow rate, but they agreed well with the measured value within a difference of two U-tubes. In the case of the plenum volume of 0.05 m³, the nitrogen reverse flow was not calculated in the region of $N_{act} \leq 20$ for 7.2c-1.2, but it was calculated in the region of $N_{act} \geq 17$ for 7.2c-1.3. For 7.2c-1.4, the flow channel with the larger flow area became the nitrogen reverse flow in cases of 19:15 and 18:16. The results overestimated the number of active U-tubes with the maximum nitrogen recirculation flow rate, but they agreed rather well with the measured value within a difference of 4 U-tubes. Compared with the steady-state analyses shown in Fig. 7 (b), solutions were obtained over a wide range of flow conditions.

Figure 10 (b) shows the calculated pressure at the SG inlet plenum. The number of active U-tubes, 34, shows the calculated pressure with a single flow channel, which was overestimated. As discussed in Fig. 9, the calculations with two flow channels and the inlet and outlet plenum volume of 0.05 m³ underestimated the primary loop pressure, especially for 7.2c-1.4. Figure 10 (b) results indicated that the flow area ratios of U-tubes in the two flow channels model and the number of active U-tubes did not greatly affect the calculated primary loop pressure. On the other hand, the gas volume in the outlet plenum, which had an uncertainty in this study, affected the calculated primary loop pressure, and the calculations with two flow channels and the inlet and outlet plenum volume of 0.02 m³ agreed well with the data.

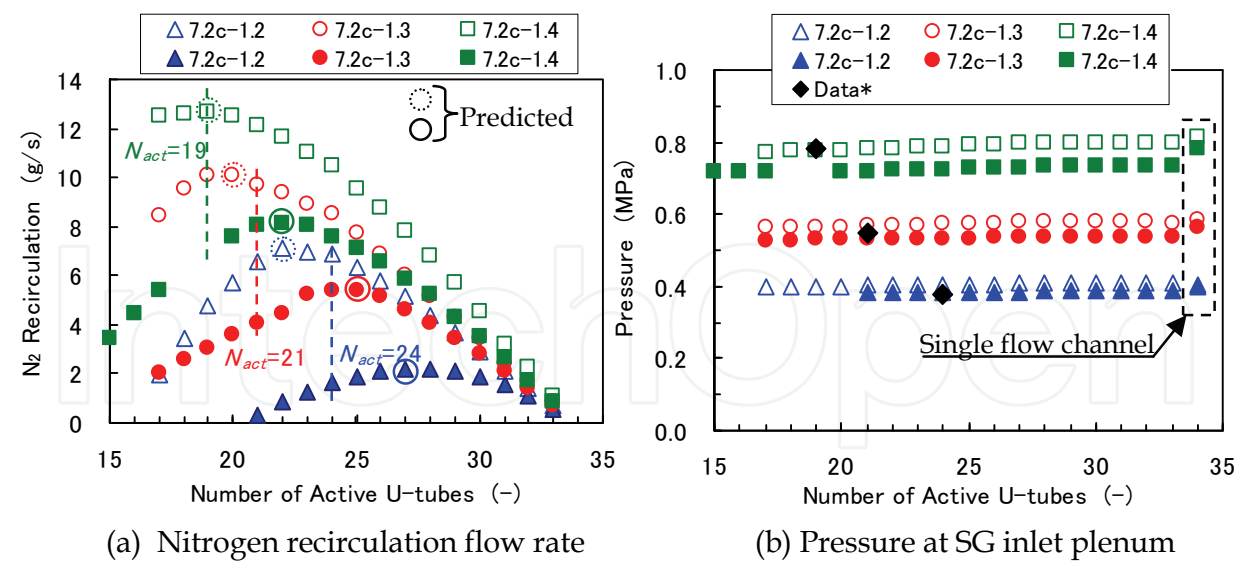


Fig. 10. Effects of number of active U-tubes as calculation parameter; open: plenum volume of 0.02 m³; closed: plenum volume of 0.05 m³; N_{act} : observed number of active U-tubes*; *Data: Noel & Deruaz (1994)

5. Transient calculations with three flow channels

In the calculations with two flow channels, we needed to perform many calculations and to assume that flow may be most stable in the case with maximum nitrogen flow rate in order to predict the number of active U-tubes. However, the assumption has not been well validated. Therefore, we did calculations using three flow channels of U-tubes in order to change the flow areas of active and passive U-tubes rather smoothly (Minami et al., 2008). We expected that the number of active U-tubes could be predicted without the assumption.

5.1 Calculation conditions

The nodalization scheme of the SG of the BETHSY tests is shown in Fig. 8. U-tubes were modeled by three flow channels, Volumes 115, 116 and 117. The calculation parameters were the plenum volume and the flow area ratio of the three flow channels. The volume of inlet and outlet plenums was 0.02 or 0.05 m³. The flow area ratio of the three flow channels was 55, 30 and 15%, 45, 35 and 20%, 45, 30 and 25% or 40, 35 and 25%. In the case of 55, 30 and 15% for example, the possible number ratios of active U-tubes were 100, 85, 70, 55, 45, 30 and 15%.

5.2 Transient behavior

Figure 11 shows gas flow rate at the U-tube inlet in three flow channels with the flow area ratios of 55, 30 and 15% (Minami et al., 2008). In the case of the plenum volume of 0.02 m³, after nitrogen injection, Volume 116 with the 30% flow area changed to nitrogen reverse flow in test 7.2c-1.2 and Volume 117 with the 15% flow area changed to nitrogen reverse flow in test 7.2c-1.3. On the other hand, in the case of the plenum volume of 0.05 m³, Volume 117 with the 15% flow area changed to nitrogen reverse flow after nitrogen injection and continued the same flow pattern. As shown in Fig. 11, the gas volume in the SG outlet plenum affected the transient behavior because nitrogen accumulated in the volume.

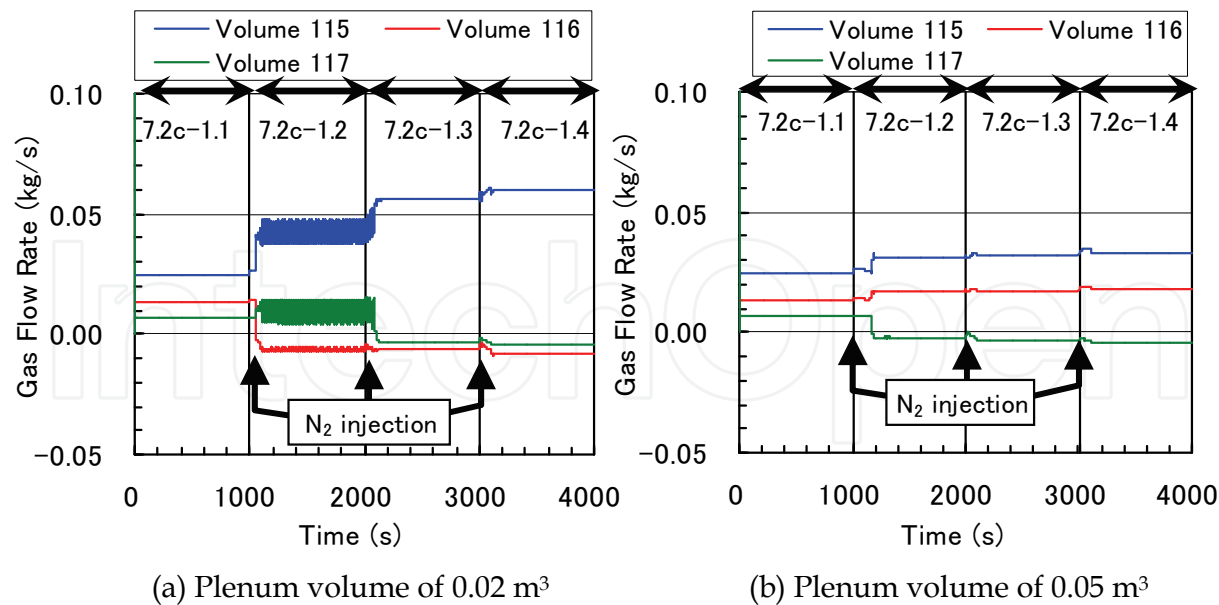


Fig. 11. Gas flow rate at U-tube inlet calculated by RELAP5/MOD3.2 using three flow channels with flow area ratios of 55, 30 and 15%

5.3 Number ratio of active U-tubes

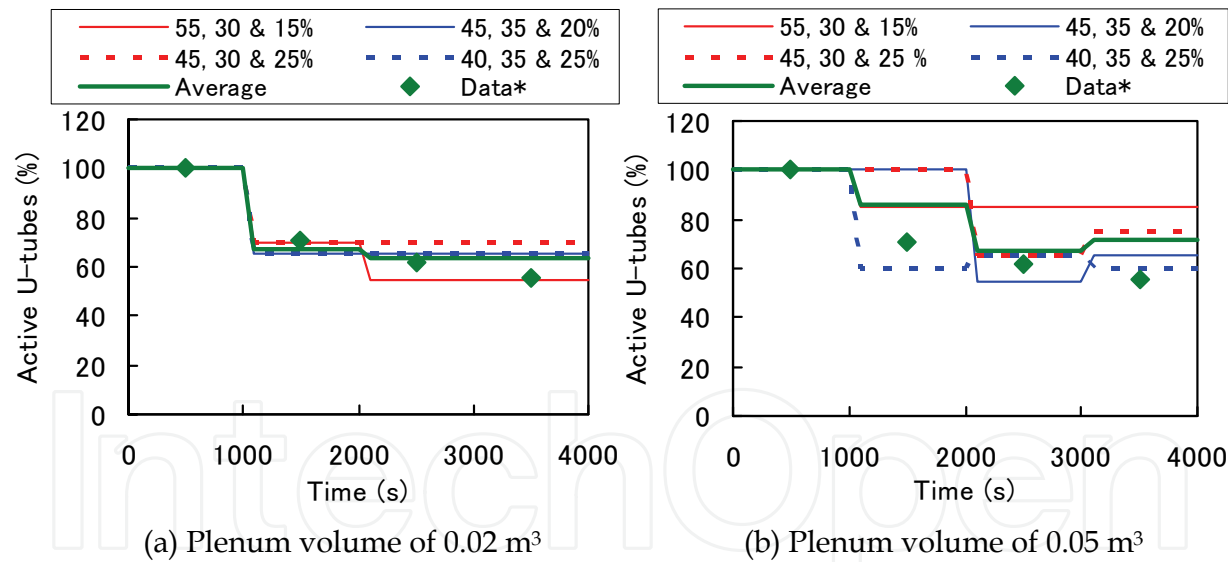


Fig. 12. Ratio of active U-tubes calculated with three flow channels

Figure 12 shows the ratio of the calculated active U-tubes (Minami et al., 2008). The calculation parameter was the flow area ratio set of U-tubes, which were 55, 30 and 15%, 45, 35 and 20%, 45, 30 and 25% or 40, 35 and 25%. In the case of the plenum volume of 0.02 m³, only Volume 116 with the medium flow area changed to nitrogen reverse flow, except for the flow area ratio set of 55, 30 and 15% shown in Fig. 11 (a), and the ratio of active U-tubes agreed with each other and with the data. Against our expectation, however, once the flow pattern changed from active flow to nitrogen reverse flow, the nitrogen reverse flow rarely returned to active flow and other channels rarely changed to nitrogen reverse flow. In the case of the plenum volume of 0.05 m³, all Volumes 115, 116 and 117 became nitrogen reverse

flow depending on the flow area ratio, and the calculated ratios of active U-tubes were scattered. The average ratios of active U-tubes were overestimated, which was similar to calculations with two flow channels shown in Fig. 10 (a), but agreed rather well with the data.

In the calculations with three flow channels, the assumption to decide the most stable state was not needed.

5.4 Discussion

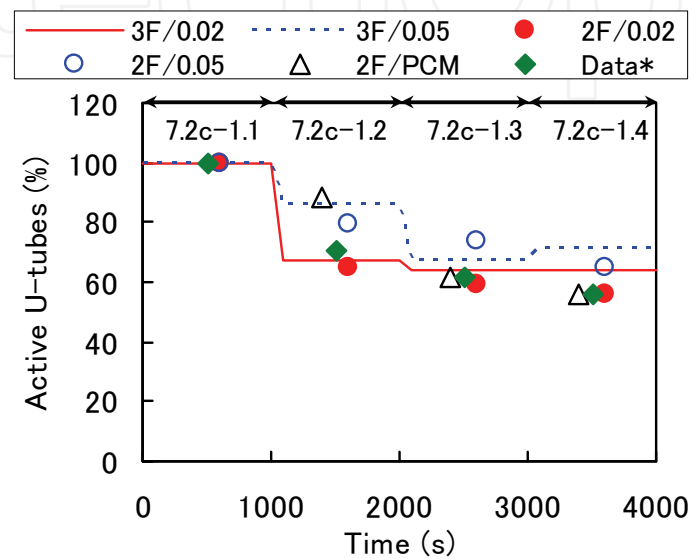


Fig. 13. Comparison of predicted ratio of active U-tubes; 2F & 3F: two and three flow channels, respectively; 0.02 & 0.05: plenum volume (m³); PCM: parallel channel model (c.f. Fig. 7 (b)); *Data: Noel & Deruaz (1994)

Figure 13 compares the ratio of active U-tubes predicted using three flow channels with that using two flow channels. The predicted ratios of active U-tubes agreed well with the data in the case with the plenum volume of 0.02 m³, but were overestimated in the case with the plenum volume of 0.05 m³. However, both cases of 0.02 and 0.05 m³ agreed well between two and three flow channels.

In the three flow channel calculations, the assumption that flow was most stable in the case with maximum nitrogen flow rate was not used. Three flow channel calculations without the assumption gave similar results to two flow channel calculations using the assumption as shown in Fig. 13. This meant that the assumption that flow was most stable in the case with the maximum nitrogen flow rate was valid.

6. Concluding remarks

In this study, condensation heat transfer of a steam-air mixture was measured using a vertical tube with the inner diameter of 19.3 mm, and an empirical correlation of condensation heat transfer coefficients for reflux condensation was derived. The correlation was incorporated into the transient analysis code RELAP5/MOD3.2 and the temperature distributions of the steam-air mixture calculated by the code for reflux condensation tests were shown to agree well with the measured results.

Different flow patterns in U-tubes observed in the reflux condensation tests 7.2c with nitrogen injection, done using the BETHSY facility with 34 U-tubes, were calculated with two flow channels of active and passive U-tubes using a parallel channel model for steady-states and RELAP5/MOD3.2 for transient calculations. In the region of low steam flow rates, the pressure in the outlet plenum became higher than the pressure in the inlet plenum due to density head of gases, and a nitrogen reverse flow occurred, which was successfully calculated by RELAP5/MOD3.2. There were many solutions with different numbers of active U-tubes with steam condensation and the predicted number of active U-tubes agreed well with the measured values based on the assumption that the flow might be most stable in the case with the maximum nitrogen recirculation flow rate. Without the assumption of the most stable state, the calculations with three flow channels gave good prediction of the ratio of active U-tubes.

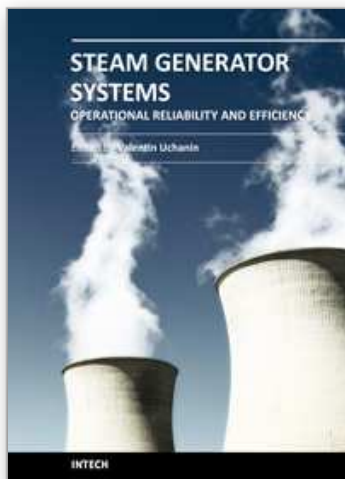
By using the proposed method (one-dimensional parallel-channel calculations), the ratio of active and passive U-tubes can be predicted even for an actual steam generator with about 3,000 U-tubes. However, it should be noted that the method can not identify the location of active U-tubes. In order to do that, three-dimensional calculations are required to evaluate the inertia effect of a steam flow into the SG inlet plenum.

7. References

- Bazin, P. (1988). *BETHSY: DATA BASE note SETH/LES/87-28*, Centre D'études Nucleaires De Grenoble, Grenoble, France.
- Chun, M. H.; Won, K. W. & Chu, I. C. (2001). An Experimental Investigation of Reflux Condensation Phenomena in Multiple U-tubes with and without Non-Condensable Gas, *Proceedings of 2001 ASME Int. Mechanical Eng. Congress and Exposition*, HTD-Vol. 369-2, pp. 194-196, New York, NY, November 2001, American Society of Mechanical Engineers, New York.
- McAdams, W. H. (1954). *Heat Transfer*, 3rd ed., McGraw-Hill, New York.
- Minami, N.; Chikusa, T. & Murase, M. (2008). RELAP5 Analyses of Thermal-Hydraulic Behavior in Steam Generator U-tubes during Reflux Condensation, *Nuclear Technology*, Vol. 164, pp. 265-277.
- Moon, Y. M.; No, H. C.; Park, H. S. & Bang, Y. S. (2000). *Assessment of RELAP5/MOD3.2 for Reflux Condensation Experiments*, NUREG/IA-0181, U. S. Nuclear Regulatory Commission, Washington, DC.
- Murase, M. & Nagae, T. (2005). Analysis of Non-condensable Gas Recirculation in Steam Generator U-tubes during Reflux Cooling, *Japanese J. of Multiphase Flow*, Vol. 19, No. 2, pp. 136-143. [in Japanese]
- Murase, M. & Suzuki, H. (1986). Countercurrent Gas/Liquid Flow in Parallel Channels Simulating a Boiling Water Reactor Core, *Nuclear Engineering and Design*, Vol. 95, pp. 79-89.
- Nagae, T.; Murase, M.; Wu, T. & Vierow, K. (2005). Evaluation of Reflux Condensation Heat Transfer of Steam-Air Mixtures under Gas-Liquid Countercurrent Flow in a Vertical Tube, *J. Nucl. Sci. Tech.*, Vol. 42, No. 1, pp. 50-57.
- Nagae, T.; Murase, M.; Chikusa, T.; Vierow, K. & Wu, T. (2007a). Reflux Condensation Heat Transfer of Steam-Air Mixtures under Turbulent Flow Conditions in a Vertical Tube, *J. Nucl. Sci. Tech.*, Vol. 44, No. 2, pp. 171-182.

- Nagae, T.; Chikusa, T.; Murase, M. & Minami, N. (2007b). Analysis of Noncondensable Gas Recirculation Flow in Steam Generator U-tubes during Reflux Condensation using RELAP5, *J. Nucl. Sci. Tech.*, Vol. 44, No. 11, pp. 1395-1406.
- Nithianandan, C. K.; Morgan, C. D.; Shah, N. H. & Miller, F. R. (1986). RELAP5/MOD2 Model for Surface Condensation in the Presence of Noncondensable Gases, *Proceedings of 8th Int. Heat Transfer Conf.*, Vol. 4, pp. 1627-1633, San Francisco, USA, August 1986.
- Noel, B. & Deruaz, R. (1994). Reflux condenser mode with non-condensable gas: assessment of Cathare against Bethsy test 7.2c, *Nuclear Engineering and Design*, Vol. 149, pp. 291-298.
- Noel, B. & Dumont, D. (1997). Effect of Non-Condensable Gas on Steam Generator Condensation Heat Transfer: BETHSY Test 10.2, *Proceedings of 5th Int. Conf. on Nuclear Eng.*, ICONE5-2536, Nice, France, May 1997.
- Ozawa, M. (1999). Flow instability problems in steam-generating tubes, *Steam power engineering: thermal and hydraulic design principles*, Ishigai, S. Ed., pp. 323-385, Cambridge University Press, Cambridge.
- The RELAP5 Development Team (1995). RELAP5/MOD3 Code Manual, NUREG/CR-5535, INEL-95/0174, Vo. 2, Idaho National Engineering Laboratory, Idaho Falls, ID.
- Vierow, K.; Nagae, T. & Wu, T. (2003). Experimental investigation of reflux condensation heat transfer in PWR steam generator tubes in the presence of non-condensable gases, *Proceedings of The 10th Int. Topical Meeting on Nuclear Thermal Hydraulics*, Seoul, Korea, October 2003.
- Wallis, G. B. (1969). *One-dimensional Two-phase Flow*, McGraw Hill, New York.
- Wallis, G. B., et al. (1981). Countercurrent Gas-Liquid Flow in Parallel Vertical Tubes, *Int. J. of Multiphase Flow*, Vol. 7, pp. 1-19.

IntechOpen



Steam Generator Systems: Operational Reliability and Efficiency

Edited by Dr. Valentin Uchanin

ISBN 978-953-307-303-3

Hard cover, 424 pages

Publisher InTech

Published online 16, March, 2011

Published in print edition March, 2011

The book is intended for practical engineers, researchers, students and other people dealing with the reviewed problems. We hope that the presented book will be beneficial to all readers and initiate further inquiry and development with aspiration for better future. The authors from different countries all over the world (Germany, France, Italy, Japan, Slovenia, Indonesia, Belgium, Romania, Lithuania, Russia, Spain, Sweden, Korea and Ukraine) prepared chapters for this book. Such a broad geography indicates a high significance of considered subjects.

How to reference

In order to correctly reference this scholarly work, feel free to copy and paste the following:

Michio Murase, Takashi Nagae and Noritoshi Minami (2011). Evaluation of Non-condensable Gas Recirculation Flow in Steam Generator U-tubes during Reflux Condensation, Steam Generator Systems: Operational Reliability and Efficiency, Dr. Valentin Uchanin (Ed.), ISBN: 978-953-307-303-3, InTech, Available from: <http://www.intechopen.com/books/steam-generator-systems-operational-reliability-and-efficiency/evaluation-of-non-condensable-gas-recirculation-flow-in-steam-generator-u-tubes-during-reflux-condensation>

INTECH
open science | open minds

InTech Europe

University Campus STeP Ri
Slavka Krautzeka 83/A
51000 Rijeka, Croatia
Phone: +385 (51) 770 447
Fax: +385 (51) 686 166
www.intechopen.com

InTech China

Unit 405, Office Block, Hotel Equatorial Shanghai
No.65, Yan An Road (West), Shanghai, 200040, China
中国上海市延安西路65号上海国际贵都大饭店办公楼405单元
Phone: +86-21-62489820
Fax: +86-21-62489821

© 2011 The Author(s). Licensee IntechOpen. This chapter is distributed under the terms of the [Creative Commons Attribution-NonCommercial-ShareAlike-3.0 License](https://creativecommons.org/licenses/by-nc-sa/3.0/), which permits use, distribution and reproduction for non-commercial purposes, provided the original is properly cited and derivative works building on this content are distributed under the same license.

IntechOpen

IntechOpen